International Journal of Solids and Structures 49 (2012) 1189–1194

Contents lists available at SciVerse ScienceDirect

International Journal of Solids and Structures

journal homepage: www.elsevier.com/locate/ijsolstr

Analytical model of thermal striping for a micro-cracked solid

M.J. Nieves [a,*], A.B. Movchan [b], I.S. Jones [a]

[a] School of Engineering, John Moores University, James Parsons Building, Byrom Street, Liverpool L3 3AF, UK
[b] Department of Mathematical Sciences, University of Liverpool, Liverpool L69 3BX, UK

ARTICLE INFO

Article history:
Received 6 July 2011
Received in revised form 23 December 2011
Available online 3 February 2012

Keywords:
Thermal striping
Stress intensity factor
Weight functions
Crack interaction
Singular perturbations
Asymptotic approximations

ABSTRACT

Using the formal asymptotic approximation of the Mode I stress intensity factor for an edge crack in a thermoelastic half plane containing several small voids obtained in [Nieves, M.J., Movchan, A.B., and Jones, I.S., 2011. Asymptotic study of a thermoelastic problem in a semi-infinite body containing a surface-breaking crack and small perforations. QJMAM 64 (3), 349–369] we investigate the effect of micro-cracks on this stress intensity factor. In numerical examples, we show how the behaviour of the stress intensity factor as a function of crack depth is affected by micro-cracks of different orientations occurring in the half space.

1. Introduction

The incomplete mixing of fluids of different temperatures, where in the mixing zone, temperatures vary randomly both temporally and spatially is known as thermal striping. Damage induced by the phenomenon of thermal striping can occur in components of pressurised water reactors and fast reactors in nuclear industry. The effect of thermal striping on edge cracks in solids, has been modelled in Jones (1997, 2003, 2005, 2006), Jones and Lewis (1994), Movchan and Jones (2006). Stress intensity factors (SIF) for edge cracks in thermoelastic solids and, in particular, their behaviour with variation of crack depth, has been determined by, amongst other methods, the weight function method (Bueckner, 1970).

The model of thermal striping for a half plane with an edge crack (Movchan and Jones, 2006), was extended in Nieves et al. (2011) to the case when the body contained several small defects of arbitrary shape. An approximation of the Mode I SIF for the edge crack was derived and, for the situation when these defects were small circular voids, numerical examples were also given. These calculations showed the effect on the SIF when the radii of these voids and their distances from the crack was varied.

There are a number of situations in engineering where the presence of micro-cracks can influence the growth of macro defects e.g. Tzimas and Papadimitrioua (2001), Lavrov et al. (2002) and Ke et al. (2006). The fatigue of solids and initiation of cracks is an important consideration in the welding of joints which are subjected to cyclic thermal loads (Thevenet et al., 2008). Identification of the conditions when cracks arise in welds with impurities and prediction of their growth is considered in Cross and Coniglio (2008) and Otegui et al. (1989). Micro-cracking in composite materials exposed to cyclic temperature was investigated in Ju et al. (2007), and it was found that high temperatures can increase the likelihood of micro-cracks occurring within the composite.

The application of the asymptotic formula for the SIF in Nieves et al. (2011) relies on the dipole matrices for each void (Movchan et al., 2002). The complex potential approach of Muskhelishvili (1953) can be used to construct these matrices, for voids of various shapes. It is possible to construct the dipole matrix for a micro-crack of finite length (Valentini et al., 1999). In Nieves et al. (2011), circular shaped voids and their effect on the SIF were modelled. In Movchan and Jones (2006) the variation of the SIF with crack depth has been investigated. Here, we use the dipole matrix for a micro-crack to investigate the effect on the SIF variation for an edge crack in a half plane.

The structure of the paper is as follows: in Section 2, we give the definition of the current problem and discuss the results of Nieves et al. (2011). The focus of Section 3 is the introduction of the model problems used in the construction of the asymptotic approximation for the Mode I SIF in a half plane with a single edge crack and micro-cracks. An outline of the proof of this approximation is provided in Section 4. In Section 5, we present numerical illustrations to show the effect of two micro-cracks on the SIF for a single edge-cracked half plane under thermal striping loading. Finally, in Section 6, we give some general conclusions of the results presented here and in Nieves et al. (2011).

2. The asymptotic model of the SIF for the thermoelastic problem

Here, we outline the existing asymptotic model for the thermal striping problem in a half plane (Movchan and Jones, 2006). In

* Corresponding author. Tel.: +44 (0) 151 231 2253.
E-mail address: M.J.Nieves@ljmu.ac.uk (M.J. Nieves).

0020-7683/$ - see front matter © 2012 Elsevier Ltd. All rights reserved.
doi:10.1016/j.ijsolstr.2012.01.003

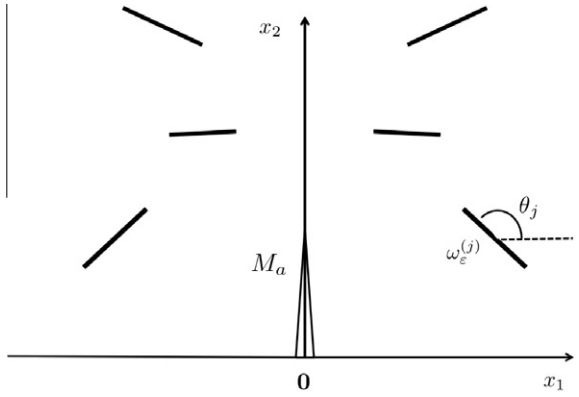

Fig. 1. A half plane with an edge crack of finite length and micro-cracks $\omega_\varepsilon^{(j)}$.We consider a symmetric Mode I loading configuration.

particular we recall a theorem (Nieves et al., 2011) which shows how the SIF maybe calculated from knowledge of the dipole matrix for any void present.

Let $\mathbb{R}^2_+ = \{\mathbf{x} \in \mathbb{R}^2 | x_2 > 0\}$ be the upper half plane with boundary $\ell = \{\mathbf{x} : x_2 = 0, x_1 \in \mathbb{R}\}$. Inside this domain we have the edge crack $M_a = M_a^+ \cup M_a^-$ with $M_a^\pm = \{\mathbf{x} \in \mathbb{R}^2_+ | x_1 = \pm 0, 0 \leqslant x_2 \leqslant a, a > 0\}$. Situated away from the boundary of the edge-cracked half plane, at a distance of $O(1)$, we also have several micro-cracks $\omega_\varepsilon^{(j)} = \{\mathbf{x} : \mathbf{x} = \varepsilon|\mathbf{x} - \mathbf{O}^{(j)}|(\cos(\theta_j), \sin(\theta_j))^T, |\mathbf{x} - \mathbf{O}^{(j)}| \leqslant b_j, -\pi < \theta_j \leqslant \pi\}$. Here, ε is a small positive parameter, $\mathbf{O}^{(j)}$ is the centre of the j^{th} micro-crack and εb_j is the half crack length. We make the assumptions that the minimum distance between each centre is $O(1)$, and the geometry of $\mathbb{R}^2_+ \setminus (\cup_{j=1}^N \omega_\varepsilon^{(j)} \cup M_a)$ is symmetric with respect to the line $x_1 = 0$ (see Fig. 1).

The scaled variable $\boldsymbol{\xi}_j = \varepsilon^{-1}(\mathbf{x} - \mathbf{O}^{(j)})$ is also used so that we can consider problems posed outside of the scaled cracks $\omega^{(j)} = \{\boldsymbol{\xi}_j : \varepsilon\boldsymbol{\xi}_j + \mathbf{O}^{(j)} \in \omega_\varepsilon^{(j)}\} \subset \mathbb{R}^2$.

Let λ and μ be the Lamé elastic moduli. Using Hooke's matrix

$$\mathcal{C} = \begin{pmatrix} \lambda + 2\mu & \lambda & 0 \\ \lambda & \lambda + 2\mu & 0 \\ 0 & 0 & 2\mu \end{pmatrix}$$

and the linear matrix function

$$\mathbf{D}(\boldsymbol{\xi}) = \begin{pmatrix} \xi_1 & 0 & 2^{-1/2}\xi_2 \\ 0 & \xi_2 & 2^{-1/2}\xi_1 \end{pmatrix}, \tag{2.1}$$

we can define the Lamé operator of two-dimensional elasticity as

$$\boldsymbol{\mathcal{L}}(\nabla_{\mathbf{x}}) := \mathbf{D}(\nabla_{\mathbf{x}})\mathcal{C}\mathbf{D}(\nabla_{\mathbf{x}})^T$$

and the corresponding differential operator of tractions $\boldsymbol{\sigma}^{(\mathbf{n})}(\nabla_{\mathbf{x}}) = (\sigma_1^{(\mathbf{n})}(\nabla_{\mathbf{x}}), \sigma_2^{(\mathbf{n})}(\nabla_{\mathbf{x}}))^T$ by

$$\boldsymbol{\sigma}^{(\mathbf{n})}(\nabla_{\mathbf{x}}) := \mathbf{D}(\mathbf{n})\mathcal{C}\mathbf{D}(\nabla_{\mathbf{x}})^T, \tag{2.2}$$

where $\mathbf{n} = (n_1, n_2)^T$ is the unit normal to the boundary under consideration.

By Γ we denote the fundamental solution of $-\boldsymbol{\mathcal{L}}(\nabla_{\mathbf{x}})$:

$$\Gamma(\mathbf{x}, \mathbf{y}) = q \begin{pmatrix} -\kappa \log|\mathbf{x} - \mathbf{y}|^2 + \frac{2(x_1 - y_1)^2}{|\mathbf{x} - \mathbf{y}|^2} & \frac{2(x_1 - y_1)(x_2 - y_2)}{|\mathbf{x} - \mathbf{y}|^2} \\ \frac{2(x_1 - y_1)(x_2 - y_2)}{|\mathbf{x} - \mathbf{y}|^2} & -\kappa \log|\mathbf{x} - \mathbf{y}|^2 + \frac{2(x_2 - y_2)^2}{|\mathbf{x} - \mathbf{y}|^2} \end{pmatrix},$$

where

$$q = \frac{\lambda + \mu}{8\pi\mu(\lambda + 2\mu)}, \quad \kappa = 3 - 4\nu, \quad \nu = \frac{\lambda}{2(\lambda + \mu)}. \tag{2.3}$$

Let $\mathbf{u}_{\varepsilon,t}$ and T be solutions of the uncoupled thermoelastic problem:

$$\left.\begin{aligned} \boldsymbol{\mathcal{L}}(\nabla_{\mathbf{x}})\mathbf{u}_{\varepsilon,t}(\mathbf{x}) &= \gamma\nabla_{\mathbf{x}}T(\mathbf{x}, t), \quad \mathbf{x} \in \mathbb{R}^2_+ \setminus (\cup_{j=1}^N \omega_\varepsilon^{(j)} \cup M_a), \\ \boldsymbol{\sigma}^{(\mathbf{n})}(\nabla_{\mathbf{x}})\mathbf{u}_{\varepsilon,t}(\mathbf{x}) &= \gamma\mathbf{n}T(\mathbf{x}, t), \quad \mathbf{x} \in \partial(\mathbb{R}^2_+ \setminus (\cup_{j=1}^N \omega_\varepsilon^{(j)} \cup M_a)), \\ \mathbf{u}_{\varepsilon,t}(\mathbf{x}) &\to \mathbf{0} \quad \text{as} \quad |\mathbf{x}| \to \infty, \end{aligned}\right\} \tag{2.4}$$

$$\left.\begin{aligned} \varkappa\Delta_{\mathbf{x}}T(\mathbf{x}, t) &= \tfrac{\partial T}{\partial t}(\mathbf{x}, t), \quad \mathbf{x} \in \mathbb{R}^2_+ \setminus M_a, \quad t > 0, \\ T(\mathbf{x}, t) &= \varphi(t), \quad x_2 = 0, x_1 \in \mathbb{R}, \quad t > 0, \\ \nabla_{\mathbf{x}}T(\mathbf{x}, t) &\to \mathbf{0} \quad \text{as } x_2 \to \infty, \quad t > 0, \end{aligned}\right\} \tag{2.5}$$

where $\mathbf{0}$ is the zero vector in $\mathbb{R}^2$, $\varkappa$ is the thermal diffusivity, $\gamma = \alpha(3\lambda + 2\mu)$, and α is the linear thermal expansion coefficient of the material occupying $\mathbb{R}^2_+ \setminus (\cup_{j=1}^N \omega_\varepsilon^{(j)} \cup M_a)$. In (2.4) t is treated as a parameter.

In Nieves et al. (2011), asymptotic approximations are obtained for the SIF $K_{\varepsilon,t}(a)$ and $\mathbf{u}_{\varepsilon,t}$ for the problem (2.4) and (2.5), under the assumptions that:

(i) $\omega_\varepsilon^{(j)}$, $j = 1, \ldots, N$, were voids, which are defined as the limit case of soft inclusions whose thermal diffusivity is the same as the diffusivity of the ambient medium,

(ii) φ is periodic in time and that T satisfies the conditions of ideal contact across the crack M_a.

As the main result of Nieves et al. (2011), we have:

Theorem. *The formal asymptotic approximation of the Mode I SIF $K_{\varepsilon,t}(a)$ associated with the problems (2.4) and (2.5) is given by*

$$\boxed{K_{\varepsilon,t}(a) \sim K_t(a) + \varepsilon^2 \sum_{k=1}^N (\mathbf{D}(\nabla_{\mathbf{x}})^T\mathbf{w}(\mathbf{x}))^T|_{\mathbf{x}=\mathbf{0}^{(k)}} \boldsymbol{\mathcal{M}}^{(k)}\boldsymbol{\mathcal{A}}_t^{(k)},} \tag{2.6}$$

where

$$\boldsymbol{\mathcal{A}}_t^{(k)} = \frac{\gamma T(\mathbf{O}^{(k)}, t)}{2(\lambda + \mu)} \begin{pmatrix} 1 \\ 1 \\ 0 \end{pmatrix} - \mathbf{D}(\nabla_{\mathbf{x}})^T\mathbf{V}_t(\mathbf{x})|_{\mathbf{x}=\mathbf{0}^{(k)}},$$

$\mathbf{V}_t$ is the solution of the unperturbed problem (2.4) and (2.5) (without defects) in the half plane with the edge crack having SIF K_t, $\mathbf{w}$ is the weight function in this domain and $\boldsymbol{\mathcal{M}}^{(j)}$ is the dipole matrix for the scaled defect.

In order to apply this theory to the current settings, we replace (i), above, with the assumption that the conditions of ideal contact across the micro-cracks $\omega_\varepsilon^{(j)}$ are also satisfied.

The SIF $K_{\varepsilon,t}$ is obtained using the weight function method (Bueckner, 1970). That is, for a loaded edge crack in a free elastic half plane $\mathbb{R}^2_+$, the Mode I SIF $\mathcal{K}_I$ is given by

$$\mathcal{K}_I(a) = 2\int_0^a (\boldsymbol{\sigma}^{(\mathbf{n})}(\nabla_{\mathbf{x}})\mathbf{u}(\mathbf{x}) \cdot \mathbf{w}(\mathbf{x}))|_{x_1=0^+}\, dx_2,$$

where $\mathbf{w}$ is the weight function for the half plane with edge crack, $\mathbf{u}$ is the displacement field produced by this loading and $x_1 = 0^+$ denotes the trace of the integrand being taken on the right-hand side of the crack where the normal to this surface is $\mathbf{n} = (-1, 0)^T$.

3. Model fields

Here we give model problems that were used in Nieves et al. (2011), to derive the asymptotic approximation for the Mode I SIF $K_{\varepsilon,t}$.

3.1. Solution of the uncoupled thermoelastic problem in the half plane with the edge crack

By $\mathbf{V}_t(\mathbf{x})$ we mean the solution of the unperturbed problem (2.4) (without the micro-cracks $\omega_\varepsilon^{(j)}$), with T as the solution of (2.5). The

SIF for the edge crack M_a corresponding to the field $\mathbf{V}_t$ will be denoted by $K_t(a)$.

Consider a half plane containing an edge crack, which is subjected to a sinusoidal thermal striping load, when

$$\varphi(t) = T_0 e^{i\omega t}, \tag{3.1}$$

where T_0 is a constant and ω is the angular frequency. Then, the temperature field T admits the form

$$T(\mathbf{x},t) = T_0 e^{-(i+1)\sqrt{\frac{\omega}{2\varkappa}}x_2 + i\omega t}.$$

The vector function $\mathbf{V}_t$ can be represented by

$$\mathbf{V}_t(\mathbf{x}) = \mathbf{u}_t(\mathbf{x}) + \mathbf{U}_t(\mathbf{x}),$$

where the solution $\mathbf{u}_t(\mathbf{x}) = (u_t^{(1)}(\mathbf{x}), u_t^{(2)}(\mathbf{x}))^T$ satisfies half plane problem (2.4) (without edge crack) and has the components

$$u_t^{(1)}(\mathbf{x}) = 0,$$

$$u_t^{(2)}(\mathbf{x}) = -\frac{T_0}{2}\sqrt{\frac{2\varkappa}{\omega}}\frac{\gamma}{\lambda+2\mu}(1-i)e^{-(i+1)\sqrt{\frac{\omega}{2\varkappa}}x_2 + i\omega t}.$$

The vector function $\mathbf{U}_t(\mathbf{x})$ then solves

$$\begin{aligned}
&\mathcal{L}(\nabla_{\mathbf{x}})\mathbf{U}_t(\mathbf{x}) = \mathbf{0}, \quad \mathbf{x} \in \mathbb{R}^2_+ \setminus \overline{M_a},\\
&\boldsymbol{\sigma}^{(\mathbf{n})}(\nabla_{\mathbf{x}})\mathbf{U}_t(\mathbf{x}) = \mathbf{0}, \quad \mathbf{x} \in \ell,\\
&\boldsymbol{\sigma}^{(\mathbf{n})}(\nabla_{\mathbf{x}})\mathbf{U}_t(\mathbf{x}) = \frac{2\mu\gamma}{\lambda+2\mu}T(\mathbf{x},t)\mathbf{n}, \quad \mathbf{x} \in M_a^{\pm},\\
&\mathbf{U}_t(\mathbf{x}) \to \mathbf{0} \quad \text{as} \quad |\mathbf{x}| \to \infty.
\end{aligned}$$

In the examples of Section 5, we use the crack tip asymptotics (Fett and Munz, 1997) for $\mathbf{U}_t$ where the SIF for this problem is given by

$$K_t(a) = -\frac{4\mu\gamma}{\lambda+2\mu}\int_0^a w_1(0^+,x_2)T(\mathbf{x},t)|_{x_1=0^+}dx_2. \tag{3.2}$$

3.2. Regular part of Neumann's tensor in a half plane with an edge crack

Let $\mathcal{H}$ be the regular part of the Neumann's tensor in $\mathbb{R}^2_+ \setminus M_a$ which is a solution of

$$\mathcal{L}(\nabla_{\mathbf{x}})\mathcal{H}(\mathbf{x},\mathbf{y}) = \mathbb{O}_2, \quad \mathbf{x} \in \mathbb{R}^2_+ \setminus M_a,$$

$$\boldsymbol{\sigma}^{(\mathbf{n})}(\nabla_{\mathbf{x}})\mathcal{H}(\mathbf{x},\mathbf{y}) = \boldsymbol{\sigma}^{(\mathbf{n})}(\nabla_{\mathbf{x}})\Gamma(\mathbf{x},\mathbf{y}), \quad \mathbf{x} \in \ell \cup M_a^+ \cup M_a^-,$$

$$\mathcal{H}(\mathbf{x},\mathbf{y}) = O(|\log|\mathbf{x}||) \quad \text{as} \quad |\mathbf{x}| \to \infty$$

for a fixed $\mathbf{y} \in \mathbb{R}^2_+ \setminus M_a$, and the components of $\mathcal{H}$ are bounded near the crack tip. Here $\mathbb{I}_2$ and $\mathbb{O}_2$ are the 2×2 identity and null matrices, respectively.

3.3. Dipole fields for the scaled cracks $\omega^{(j)}$, $j = 1,\dots,N$

Let $\mathcal{W}^{(j)}$ be a 2×3 matrix satisfying

$$\mathcal{L}(\nabla_{\xi_j})\mathcal{W}^{(j)}(\xi_j) = \mathbb{O}_{2\times 3}, \quad \xi_j \in \mathbb{R}^2 \setminus \omega^{(j)},$$

$$\boldsymbol{\sigma}^{(\mathbf{n})}(\nabla_{\xi_j})\mathcal{W}^{(j)}(\xi_j) = \mathbf{D}(\mathbf{n})\mathcal{C}, \quad \xi_j \in \partial\omega^{(j)}, \tag{3.3}$$

$$\mathcal{W}^{(j)}(\xi_j) = O(|\xi_j|^{-1}) \quad \text{as} \quad |\xi_j| \to \infty, \tag{3.4}$$

with $\mathbb{O}_{2\times 3}$ being the 2×3 null matrix. Here, (3.4) is a consequence of the balance conditions

$$\int_{\partial\omega^{(j)}} \boldsymbol{\sigma}^{(\mathbf{n})}(\nabla_{\xi_j})\mathcal{W}^{(j)}(\xi_j)dS_{\xi_j} = \mathbb{O}_{2\times 3},$$

$$\int_{\partial\omega^{(j)}} \left\{\xi_{j1}\sigma_2^{(\mathbf{n})}(\nabla_{\xi_j})\mathcal{W}^{(j,p)}(\xi_j) - \xi_{j2}\sigma_1^{(\mathbf{n})}(\nabla_{\xi_j})\mathcal{W}^{(j,p)}(\xi_j)\right\}dS_{\xi_j} = 0, \quad p = 1,2,3.$$

The columns $\mathcal{W}^{(j,i)}$, $j = 1,2,3$ have the interpretation as the dipole fields for the crack $\omega^{(j)}$.

3.3.1. The dipole matrix for a finite crack

The dipole matrix for the crack $\omega^{(j)}$ with scaled half length b_j and at angle of θ_j with the horizontal axis, is denoted by $\mathcal{M}^{(j)} = [\mathcal{M}_{ik}^{(j)}]_{i,k=1}^3$. From Valentini et al. (1999), this matrix has the representation:

$$\mathcal{M}^{(j)} = -\frac{b_j^2\pi(\lambda+2\mu)}{4\mu}\begin{pmatrix} \Xi_j+\Theta_j+\Sigma_j & \Xi_j-\Theta_j & \Lambda_j \\ \Xi_j-\Theta_j & \Xi_j+\Theta_j-\Sigma_j & \Lambda_j \\ \Lambda_j & \Lambda_j & 2\Theta_j \end{pmatrix}, \tag{3.5}$$

where

$$\Theta_j = \frac{2\mu^2}{\lambda+\mu},\ \ \Xi_j = 2(\lambda+\mu),\ \ \Sigma_j = -4\mu\cos(2\theta_j),\ \ \Lambda_j = -2\sqrt{2}\mu\sin(2\theta_j).$$

It is clear that (3.5) is symmetric and in Movchan et al. (2002) it is shown that this matrix is negative definite and characterises the increment in energy in the infinite plane when perturbed by a crack at the origin. It can also be used to describe the far-field behaviour of the matrix $\mathcal{W}^{(j)}$ in (3.4):

Lemma 1. *For $|\xi_j| \gg 1$, the matrix $\mathcal{W}^{(j)}$ admits the asymptotic representation*

$$\mathcal{W}^{(j)}(\xi_j) = -(\mathbf{D}(\nabla_{\xi_j})^T\Gamma(\xi_j,\mathbf{0}))^T\mathcal{M}^{(j)} + O(|\xi_j|^{-2}).$$

3.4. The weight function for a half plane with an edge crack

In accordance with Bueckner (1970) and Nieves et al. (2011), when evaluating the SIF $K_{\varepsilon,t}(a)$, we use the weight function $\mathbf{w} = (w_1,w_2)^T$ for the edge-cracked half plane which satisfies

$$\mathcal{L}(\nabla_{\mathbf{x}})\mathbf{w}(\mathbf{x}) = \mathbf{0}, \quad \mathbf{x} \in \mathbb{R}^2_+ \setminus M_a,$$

$$\boldsymbol{\sigma}^{(\mathbf{n})}(\nabla_{\mathbf{x}})\mathbf{w}(\mathbf{x}) = \mathbf{0}, \quad \mathbf{x} \in \ell \cup M_a^+ \cup M_a^-, \tag{3.6}$$

$$\mathbf{w}(\mathbf{x}) \to \mathbf{0} \quad \text{as} \quad |\mathbf{x}| \to \infty, \tag{3.7}$$

$$\mathbf{w}(\mathbf{x}) = O(|\mathbf{x}-\mathbf{a}|^{-1/2}), \text{as} \quad |\mathbf{x}-\mathbf{a}| \to 0,$$

where $\mathbf{a}$ is the position of the crack tip. Since we consider a symmetric Mode I configuration, we only require the first component of $\mathbf{w}$. An approximation of this component on the crack M_a (see Hartranft and Sih, 1973) is given by

$$w_1(0^+,x_2) = \frac{(1+f(x_2/a))}{\sqrt{a^2-x_2^2}}\sqrt{\frac{a}{\pi}}, \tag{3.8}$$

where

$$f(y) = (1-y^2)(0.2945 - 0.3912y^2 + 0.7685y^4 - 0.9942y^6 + 0.5094y^8).$$

3.5. Neumann's tensor for the half plane

The Neumann's tensor G for the half plane is a solution of

$$\mathcal{L}(\nabla_{\mathbf{x}})G(\mathbf{x},\mathbf{y}) + \delta(\mathbf{x}-\mathbf{y})\mathbb{I}_2 = \mathbb{O}_2, \quad \mathbf{x} \in \mathbb{R}^2_+,$$

$$\boldsymbol{\sigma}^{(\mathbf{n})}(\nabla_{\mathbf{x}})G(\mathbf{x},\mathbf{y}) = \mathbb{O}_2, \quad \text{for} \quad x_2 = 0,$$

where $\mathbf{y} \in \mathbb{R}^2_+$, and G has the logarithmic growth at infinity. This tensor can be written as

$$G(\mathbf{x},\mathbf{y}) = \Gamma(\mathbf{x},\mathbf{y}) - H(\mathbf{x},\mathbf{y}), \tag{3.9}$$

where $H(\mathbf{x},\mathbf{y}) = [H_{ij}(\mathbf{x},\mathbf{y})]_{i,j=1}^2$ is the regular part, and its components are (see Sheremet, 2002):

$$\begin{aligned}
H_{11}(\mathbf{x},\mathbf{y}) &= -2q\left\{-\left[\kappa+\frac{2\mu^2}{(\lambda+\mu)^2}\right]\log|\mathbf{x}-\overline{\mathbf{y}}| + \frac{(x_1-y_1)^2}{|\mathbf{x}-\overline{\mathbf{y}}|^2}\right.\\
&\quad \left. -\frac{2\mu}{\lambda+\mu}\frac{(x_2+y_2)^2}{|\mathbf{x}-\overline{\mathbf{y}}|^2} - \frac{2x_2y_2}{|\mathbf{x}-\overline{\mathbf{y}}|^2} + \frac{4x_2y_2(x_2+y_2)^2}{|\mathbf{x}-\overline{\mathbf{y}}|^4}\right\},\\
H_{21}(\mathbf{x},\mathbf{y}) &= 2q\left\{-\kappa\frac{(x_1-y_1)(x_2-y_2)}{|\mathbf{x}-\overline{\mathbf{y}}|^2} + \frac{4x_2y_2(x_2+y_2)(x_1-y_1)}{|\mathbf{x}-\overline{\mathbf{y}}|^4}\right.\\
&\quad \left. +\frac{2\mu(\lambda+2\mu)}{(\lambda+\mu)^2}\arctan\left\{\frac{x_2+y_2}{x_1-y_1}\right\}\right\},\\
H_{12}(\mathbf{x},\mathbf{y}) &= 2q\left\{-\kappa\frac{(x_1-y_1)(x_2-y_2)}{|\mathbf{x}-\overline{\mathbf{y}}|^2} - \frac{4x_2y_2(x_2+y_2)(x_1-y_1)}{|\mathbf{x}-\overline{\mathbf{y}}|^4}\right.\\
&\quad \left. -\frac{2\mu(\lambda+2\mu)}{(\lambda+\mu)^2}\arctan\left\{\frac{x_2+y_2}{x_1-y_1}\right\}\right\},\\
H_{22}(\mathbf{x},\mathbf{y}) &= -2q\left\{-\left[\kappa+\frac{2\mu^2}{(\lambda+\mu)^2}\right]\log|\mathbf{x}-\overline{\mathbf{y}}| + \kappa\frac{x_2^2+y_2^2}{|\mathbf{x}-\overline{\mathbf{y}}|^2}\right.\\
&\quad \left. +\frac{4x_2y_2}{|\mathbf{x}-\overline{\mathbf{y}}|^2}\left[\frac{(x_2+y_2)^2}{|\mathbf{x}-\overline{\mathbf{y}}|^2}+\frac{\mu}{\lambda+\mu}\right]\right\},
\end{aligned} \tag{3.10}$$

where $\overline{\mathbf{y}} = (y_1,-y_2)^T$ is the image point which lies outside $\mathbb{R}^2_+$.

4. Asymptotic algorithm for $K_{\varepsilon,t}$

4.1. The thermoelastic field in $\mathbb{R}^2_+ \setminus (\cup_{j=1}^N \omega_\varepsilon^{(j)} \cup M_a)$

The method of obtaining the approximation for $K_{\varepsilon,t}$, relies on the approximation of the thermoelastic field $\mathbf{u}_{\varepsilon,t}$ contained in the next lemma:

Lemma 2. *The formal asymptotic approximation of the displacement field $\mathbf{u}_{\varepsilon,t}$ of the thermoelastic problem (2.4) and (2.5) is given by*

$$\begin{aligned}
\mathbf{u}_{\varepsilon,t}(\mathbf{x}) &\sim \mathbf{V}_t(\mathbf{x}) + \varepsilon\sum_{k=1}^N \{\mathcal{W}^{(k)}(\xi_k)\\
&\quad - \varepsilon(\mathbf{D}(\nabla_{\mathbf{z}})^T\mathcal{H}(\mathbf{x},\mathbf{z})^T)^T|_{\mathbf{z}=\mathbf{O}^{(k)}}\mathcal{M}^{(k)}\}\mathcal{A}_t^{(k)},
\end{aligned} \tag{4.1}$$

where

$$\mathcal{A}_t^{(k)} = \frac{\gamma T(\mathbf{O}^{(k)},t)}{2(\lambda+\mu)}\begin{pmatrix}1\\1\\0\end{pmatrix} - \mathbf{D}(\nabla_{\mathbf{x}})^T\mathbf{V}_t(\mathbf{x})|_{\mathbf{x}=\mathbf{O}^{(k)}}. \tag{4.2}$$

The detailed proof of this can be found in Section 4 of Nieves et al., 2011.

4.2. The SIF $K_{\varepsilon,t}$

The formal argument leading to (2.6) uses the weight function method and begins with identifying those terms in (4.1) which contribute to the approximation of the SIF $K_{\varepsilon,t}$ for the edge crack in the half plane with micro-cracks, i.e. we look for asymptotics of $O(\sqrt{r})$ as we allow $\mathbf{x}\to\mathbf{a}$. In this case, the only fields in (4.1) which produce this asymptotic behaviour are

$$\mathbf{V}_t(\mathbf{x}) \quad \text{and} \quad P^{(k)}(\mathbf{x}) = -(\mathbf{D}(\nabla_{\mathbf{z}})^T\mathcal{H}(\mathbf{x},\mathbf{z})^T)^T|_{\mathbf{z}=\mathbf{O}^{(k)}}\mathcal{M}^{(k)}\mathcal{A}_t^{(k)},$$
$k = 1,\dots,N$.

Table 1
Material properties of stainless steel at $\sim 500^\circ$C.

Thermal conductivity	20.3 W/(°C m)
Specific heat	570 J/(°C kg)
Youngs modulus	163 GPa
Poisson's ratio	0.3
Coefficient of linear expansion	2.0×10^{-5}/(°C)
Mass density	7760 kg/ m^3

The field $\mathbf{V}_t$ produces the unperturbed SIF $K_t(a)$ for the edge crack in the half plane, and let the SIF produced by $P^{(i)}$ be $K^{(i)}(a)$. Allowing $\mathbf{x}\to\mathbf{a}$ in (4.1) and using the crack tip asymptotics of these fields (Fett and Munz, 1997), we obtain

$$\frac{K_{\varepsilon,t}(a)r^{1/2}}{4\mu\sqrt{2\pi}}\mathbf{\Phi}(\mathbf{x}/|\mathbf{x}|) \sim \frac{r^{1/2}}{4\mu\sqrt{2\pi}}\left(K_t(a)+\varepsilon^2\sum_{i=1}^N K^{(i)}(a)\right)\mathbf{\Phi}(\mathbf{x}/|\mathbf{x}|),$$

with $r = |\mathbf{x}-\mathbf{a}|$ and $\mathbf{\Phi}$ is a function of the polar angle associated with the crack tip. The above implies that

$$K_{\varepsilon,t}(a) \sim K_t(a) + \varepsilon^2\sum_{i=1}^N K^{(i)}(a). \tag{4.3}$$

The SIF $K_t(a)$ is given in (3.2) and in Nieves et al. (2011), using arguments of linear superposition, it has been shown that:

$$\begin{aligned}
\sum_{i=1}^N K^{(i)}(a) &= 2\sum_{i=1}^N\int_0^a w_1(0^+,x_2)\sigma_{11}[(\mathbf{D}(\nabla_{\mathbf{z}})^T G(\mathbf{x},\mathbf{z})^T)^T|_{\mathbf{z}=\mathbf{O}^{(i)}}\\
&\quad \times \mathcal{M}^{(i)}\mathcal{A}_t^{(i)}]|_{x_1=0^+}dx_2,
\end{aligned} \tag{4.4}$$

where for a vector field $\mathbf{u} = (u_1,u_2)^T$,

$$\sigma_{ij}(\mathbf{u}) = \lambda(\nabla\cdot\mathbf{u})\delta_{ij} + \mu(u_{i,j}+u_{j,i})$$

and δ_{ij} is the Kronecker delta. By applying the Betti formula, with $\mathbf{w}$ and G in $\mathbb{R}^2_+\setminus M_a$ (Nieves et al., 2011), it is possible to show that (4.4) is equal to

$$\sum_{i=1}^N K^{(i)}(a) = \sum_{i=1}^N(\mathbf{D}(\nabla_{\mathbf{x}})^T\mathbf{w}(\mathbf{x}))^T|_{\mathbf{x}=\mathbf{O}^{(i)}}\mathcal{M}^{(i)}\mathcal{A}_t^{(i)}.$$

Substituting this in (4.3) gives (2.6).

5. The case of two micro-cracks

In Nieves et al. (2011), examples are presented which show the effect on the maximum amplitude of the stress intensity factor $K_t(a)$, for the edge crack in a stainless steel half plane, when small circular voids are present in the body. In particular, the interaction between the edge crack and small voids with different radii and at various distances from the crack were examined. Good agreement between the results based on the asymptotic approximation for the SIF and those given by finite element analysis was found. Here, we will present a similar example for the case of interaction between the edge crack and micro-cracks. We demonstrate how the orientation of the micro-cracks influences the maximum SIF.

5.1. Description of the geometry for two micro-cracks

Following Nieves et al. (2011), in this example we model an elastic half plane, containing an edge crack and micro-cracks, using the material properties of stainless steel. These properties are given in Table 1.

We consider two micro-cracks $\omega_\varepsilon^{(\pm)}$, in the edge-cracked half plane, with centres $\mathbf{O}^{(\pm)} = (\pm3\text{ mm},5\text{ mm})^T$ and length 3 mm. The angle between the axis of the crack $\omega_\varepsilon^{(+)}$ and the x_1-axis is denoted

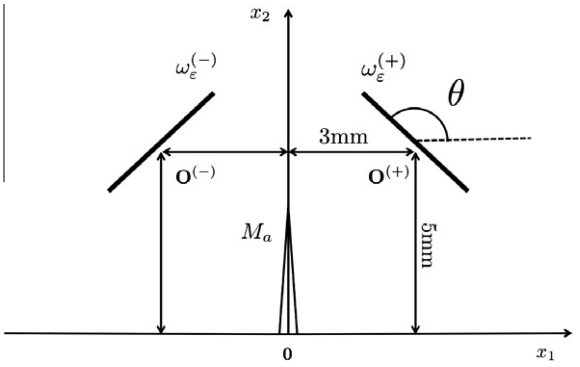

Fig. 2. A half plane containing an edge crack and two micro-cracks $\omega_\varepsilon^{(\pm)}$ with length 3mm and centres $\mathbf{O}^{(\pm)} = (\pm 3\text{mm}, 5\text{mm})^T$. The micro-cracks $\omega_\varepsilon^{(\pm)}$ are at angles of $\pm\theta$ with the x_1-axis.

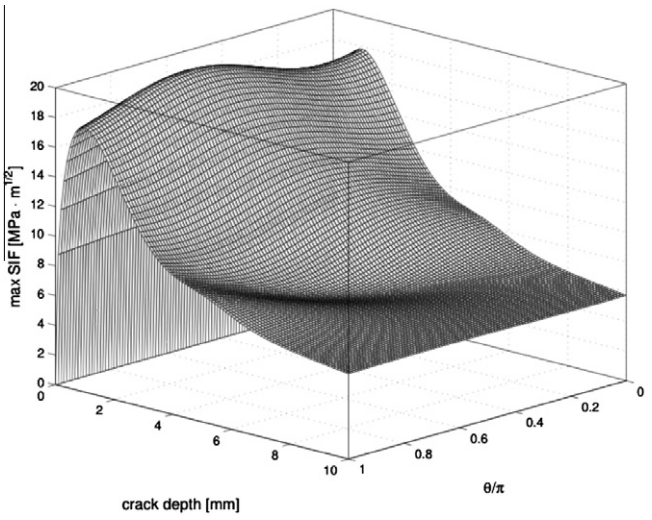

Fig. 3. A surface plot of the amplitude of the SIF $K_{\varepsilon,t}$ against edge crack depth and the normalised angle of orientation of the micro-cracks with length 3 mm and centres $\mathbf{O}^{(\pm)} = (\pm 3\text{mm}, 5\text{mm})^T$, for the case when $\varepsilon = 0.5$.

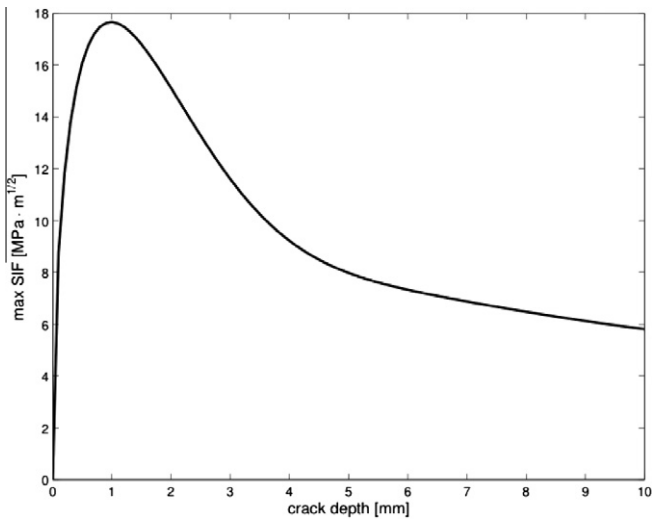

Fig. 4. A plot of the amplitude of the unperturbed SIF K_t against edge crack depth.

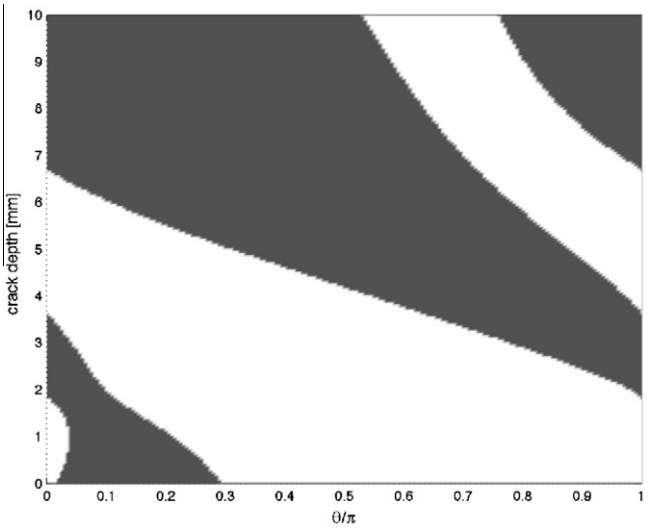

Fig. 5. The difference between the amplitude of the perturbed and unperturbed SIF against edge crack depth and the angle of orientation of the micro-cracks with length 3 mm and centres $\mathbf{O}^{(\pm)} = (\pm 3\text{ mm}, 5\text{ mm})^T$. Here, the small parameter $\varepsilon = 0.5$. Shaded regions indicate areas of lower amplitude of the SIF relative to the amplitude of the unperturbed SIF, whereas the unshaded regions represent a higher amplitude of the SIF.

by θ (see Fig. 2). We note that this diagram corresponds to an advance of the pre-existing crack, the question of crack initiation is not addressed here.

The small parameter $\varepsilon = 0.5$ is defined as the ratio of the common micro-crack half length to the minimum distance from the centres of these defects to the x_1 and x_2 axes. In (3.1) we set $T_0 = 100^\circ$C and $\omega = 2\pi$.

Combining (3.2) and (4.4) in (4.3) we have

$$K_{\varepsilon,t}(a) \sim -\frac{4\mu\gamma}{\lambda+2\mu}\int_0^a w_1(0^+,x_2)T(\mathbf{x},t)|_{x_1=0^+}\,dx_2 + 2\varepsilon^2\sum_{\pm}\int_0^a w_1(0^+,x_2)\sigma_{11}[(\mathbf{D}(\nabla_{\mathbf{z}})^T G(\mathbf{x},\mathbf{z})^T)^T|_{\mathbf{z}=\mathbf{O}^{(\pm)}}\boldsymbol{\mathcal{M}}^{(\pm)}\boldsymbol{\mathcal{A}}_t^{(\pm)}]|_{x_1=0^+}\,dx_2, \tag{5.1}$$

where the approximation to the weight function (3.8) along the line of the crack is used here, the constant vector $\boldsymbol{\mathcal{A}}_t^{(\pm)}$ has the representation (4.2), the dipole matrix $\boldsymbol{\mathcal{M}}^{(\pm)}$ for a finite crack appears in (3.5), the components of G are given by (3.9) and (3.10).

5.2. Numerical results

In this section, we analyse the amplitude of the SIF under sinusoidal striping for an edge crack in a half plane containing two micro-cracks. Fig. 3 shows the surface plot of the amplitude of the SIF as a function of crack depth (a) and the angle of orientation of the crack (θ/π). This gives the amplitude of the SIF as we rotate the micro-cracks through 180°, at various edge crack depths in the region $0 \leqslant a \leqslant 10$mm. For comparison, in Fig. 4, we also provide the plot of the unperturbed amplitude of the SIF $K_t(a)$. For edge crack depths in the region $0 \leqslant a \leqslant 8$mm one can see, by comparing Figs. 3 and 4, a visible perturbation in the amplitude of the SIF $K_t(a)$ when two micro-cracks are present in the body, with $0 \leqslant \theta < \pi$. For crack depths greater than 8 mm, the effect of micro-cracks on the amplitude of the SIF diminishes. In particular, when $0.7 \leqslant \theta/\pi \leqslant 0.8$, at a crack depth of approximately 1 mm, we have a noticeable increase to the maximum of the unperturbed amplitude of the SIF. Also in Fig. 3, at approximately the same crack depth and when $0.1 \leqslant \theta/\pi \leqslant 0.2$, we have a saddle point.

In Fig. 5, we show the difference between the unperturbed amplitude of the SIF $K_t(a)$ and the amplitude of the SIF $K_{\varepsilon,t}(a)$ as

a function of crack depth and angle of orientation of the cracks. On this figure, the shaded regions indicate a decrease in the amplitude of the SIF relative to the amplitude of the SIF $K_t(a)$ and unshaded regions represent an increase to the amplitude of the SIF relative to the amplitude of SIF $K_t(a)$ when the micro-cracks are present.

It can be seen that in between approximately $\theta = 0.3\pi$ and $\theta = 0.5\pi$, the presence of micro-cracks "ahead of" the main edge crack encourage potential crack growth since the amplitude of the SIF is increased. Conversely, when the crack tip of the edge crack is deeper into the half space than the micro-cracks, the amplitude of the SIF is decreased, leading to less likelihood of potential crack growth. Analogous behaviour was found in Nieves et al. (2011) and Thomas et al. (2000) for circular voids. For other orientations the behaviour is more complex with regions of enhanced and reduced potential for crack growth.

Similar complex behaviour, where micro-cracks "ahead of" the main crack tip may reduce the potential for crack growth for embedded main cracks has been observed in Tamuzs and Petrova (1999) and Tamuzs et al. (1994).

6. Conclusions

In Nieves et al. (2011) the model of thermal striping of an elastic half-plane containing an edge crack and small defects was analysed. Asymptotic formulae for the Mode I SIF for the edge crack was obtained, and for a configuration involving a symmetric distribution of small circular voids about the axis of the edge crack, the behaviour of this stress intensity factor was investigated. In the case of two circular holes, results showed that when positioned ahead of the crack tip, these holes brought an increase to the value of the stress intensity factor, indicating an increase for potential crack growth. For edge cracks deeper than the circular holes, the SIF for this crack decreased.

We have also investigated the behaviour of the SIF for the edge crack when micro-cracks are located in the thermally striped half plane. It was shown that compared to the case when circular holes are located in the half plane, it is possible to find orientations of the micro-cracks such that the potential for crack arrest increases when the micro-cracks are located ahead of the crack. Similarly, micro-cracks of a particular orientation may also cause the edge crack to grow, when these micro-cracks are situated behind the tip of the edge crack, and as noted above, examples of this behaviour can be found in Tamuzs et al. (1994) and Tamuzs and Petrova (1999).

These numerical simulations, based on the asymptotic formula for the Mode I SIF of the edge crack, also indicate that it is possible to identify configurations of defects inside the half-plane which can greatly reduce the potential for edge crack growth. The asymptotic formula for the SIF is applicable to a wide variety of shapes for the internal defects, provided the dipole matrix for elastic defect is known (Movchan et al., 2002; Nieves et al., 2011).

References

Bueckner, H.F., 1970. A novel principle for the computation of stress intensity factors. ZAMM 50 (9), 529–546.

Cross, C.E., Coniglio, N., 2008. Weld solidification cracking: critical conditions for crack initiation and growth. Hot Cracking Phenomena in Welds II. Springer-Verlag, Berlin, Heidelberg.

Fett, T., Munz, D., 1997. Stress Intensity Factors and Weight Functions. Advances in Fracture Series. Computational Mechanics Publications.

Hartranft, R.J., Sih, G.C., 1973. Alternating method applied to edge and surface crack problems. In: Sih, G.C. (Ed.), Methods of Analysis of Solutions of Crack Problems, Mechanics of Fracture, vol. 1. Nordhoff, Leyden, Netherlands.

Jones, I.S., 1997. The frequency response method of thermal striping for cylindrical geometries. Fatigue Fract. Eng. Mater. Struct. 20 (6), 871–882.

Jones, I.S., 2003. Small edge crack in a semi-infinite solid subjected to thermal stratification. Theoret. Appl. Fract. Mech. 39, 7–21.

Jones, I.S., 2005. Impulse response model of thermal striping for hollow cylindrical geometries. Theoret. Appl. Fract. Mech. 43 (1), 77–88.

Jones, I.S., 2006. Thermal striping fatigue damage in multiple edge-cracked geometries. Fatigue Fract. Eng. Mater. Struct. 29 (2), 123–134.

Jones, I.S., Lewis, M.W.J., 1994. A frequency response method for calculating stress intensity factors due to thermal striping loads. Fatigue Fract. Eng. Mater. Struct. 17 (6), 709–720.

Ju, J., Morgan, R.J., Creasy, T.S., Shin, E.E., 2007. Transverse cracking of M40J/PMR-II-50 composites under thermal-mechanical loading: Part II experiment and analytical investigation. J. Compos. Mater. 41 (9), 1067–1086.

Ke, P.L., Wang, Q.M., Gong, J., Sun, C., Zhou, Y.C., 2006. Progressive damage during thermal shock cycling of D-gun sprayed thermal barrier coatings with hollow spherical ZrO_2 – $8Y_2O_3$. Materials Science and Enginering A 435-436, 228–236.

Lavrov, A., Vervoort, A., Wevers, M., Napier, J.A.L., 2002. Experimental and numerical study of the Kaiser effect in Brazilian tests with disk rotation. International Journal of Rock Mechanics and Mining Sciences 39 (3), 287–302.

Movchan, A.B., Jones, I.S., 2006. Asymptotic and numerical study of a surface breaking crack subject to a transient thermal load. Acta Mech. Sin. 22 (1), 22–27.

Movchan, A.B., Movchan, N.V., Poulton, C.G., 2002. Asymptotic Models of Fields in Dilute and Densely Packed Composites. Imperial College Press.

Muskhelishvili, N.I., 1953. Some Basic Problems of the Mathematical Theory of Elasticity. Nordhoff, Groningen.

Nieves, M.J., Movchan, A.B., Jones, I.S., 2011. Asymptotic study of a thermoelastic problem in a semi-infinite body containing a surface-breaking crack and small perforations. Quart. J. Mech. Appl. Math. 64 (3), 349–369.

Otegui, J.L., Kerr, H.W., Burns, D.J., Mohaupt, U.H., 1989. Fatigue crack initiation from defects at weld toes in steel. Int. J. Press. Vessels Piping 38 (5), 385–417.

Sheremet, V.D., 2002. Handbook on Green's Functions and Matrices. WIT press.

Tamuzs, V., Petrova, V., 1999. Modified model of macro-microcrack interaction. Theoret. Appl. Fract. Mech. 32 (2), 111–117.

Tamuzs, V., Petrova, V., Romalis, N., 1994. Thermal fracture of macrocrack with closure as influenced by microcracks. Theoret. Appl. Fract. Mech. 21, 207–218.

Thevenet, D., Lautrou, N., Cognard, J.Y., 2008. Fatigue crack initiation in naval welded joints: experimental and numerical approaches. Proc. Appl. Math. Mech. 8, 10243–10244.

Thomas, S.B., Mhaiskar, M.J., Sethuraman, R., 2000. Stress intensity factors for circular hole and inclusion using finite element alternating method. Theoret. Appl. Fract. Mech. 33 (2), 73–81.

Tzimas, E., Papadimitrioua, G., 2001. Cracking mechanisms in high temperature hot-dip galvanized coatings. Surf. Coatings Technol. 145 (1–3), 176–185.

Valentini, M., Serkov, K., Bigoni, D., Movchan, A.B., 1999. Crack propagation in a brittle elastic material with defects. J. Appl. Mech. 66 (1), 79–86.